science.sciencemag.org/content/369/6509/1378/suppl/DC1

Supplementary Materials for

Long-term forest degradation surpasses deforestation in the Brazilian Amazon

Eraldo Aparecido Trondoli Matricardi*, David Lewis Skole*, Olívia Bueno Costa, Marcos Antonio Pedlowski, Jay Howard Samek, Eder Pereira Miguel

*Corresponding author. Email: ematricardi@gmail.com (E.A.T.M.); skole@msu.edu (D.L.S.)

Published 11 September 2020, *Science* **369**, 1378 (2020)
DOI: 10.1126/science.abb3021

This PDF file includes:

Materials and Methods

Definition of the Study Area

This analysis covers the entire Brazilian Legal Amazon, in which we term the Brazilian Amazon (BA). The Brazilian Legal Amazon is a political and administrative region in Brazil created by the Federal Law n.1806 in 1953. It encompasses a territory of approximately 5 million square kilometers within the Amazon basin that includes the Brazilian states of Acre, Amapá, Amazonas, Pará, Rondônia, Roraima, and part of Mato Grosso, Maranhão, and Tocantins. We analyzed satellite data for the entire BA. Landsat satellite imagery for all World Reference System II path/row combinations. We used all Landsat scenes for the entire Brazilian Amazon for each Observation Year. There is a subset of 79 path-row locations where logging or burned areas were detected in satellite data and we used those images for digital analysis and spatial database construction of logged and burned areas. For logging and burned areas we analyzed approximately 600 Landsat scenes within the BA (553 images comprising 7 observation years in 79 path row stacks of images, plus additional images used to improve image quality in specific locations or phenology). For edge analysis, isolated forest analysis and deforestation the entire BLA was mapped digitally. Landsat images showing high percentage of clouds were replaced by images acquired in the previous or following year of analysis. Only eight scenes with high percentage of clouds had to be replaced by images of the closest years. This fore and aft compositing procedure did not substantially reduce the area assessed for logging and understory fire. However, areas of selective logging or understory fire may have been slightly underestimated in the 2014 observation due to high cloud cover in some of the Landsat images. Analysis was conducted only for changes observed in closed forests and does not include analysis of changes in cerrado or other vegetation covers. Only forest areas were included for mapping of edges and isolated forest fragments.

Remote Sensing and GIS Datasets Used in the Analysis

Landsat imagery were obtained from the National Institute of Space Research (INPE), the United States Geological Survey (USGS) Earth Resources Observation and Science (EROS) Data Center (EDC), and the Tropical Rain Forest Information Center (TRFIC) at Michigan State University. Each Landsat image was radiometrically corrected for physical reflectance values for top of atmosphere (TOA) using the metadata provided by the TRFIC and USGS and the ENVI® 5.0 software package. Each Landsat image was geometrically corrected using ground control points acquired in the field using a Global Positioning System (GPS) or reference maps (topomaps) obtained from the Brazilian Institute of Geography and Statistic (IBGE). When needed, Landsat scenes were geometrically corrected using three or six control points and the nearest neighbor re-sampling technique to rectify them. Geometric correction was accepted only if RMS was less than 0.5 pixels. Deforestation spatial datasets (digital maps) for 1992, 1996, and 1999 were acquired from the TRFIC (*36*). Deforestation datasets for 2003, 2006, 2010, 2014, and 2018 were obtained from the Amazon Deforestation Monitoring Project (PRODES) conducted by the National Institute for Space Research (INPE) in Brazil (23). These digital deforestation datasets from TRFIC (*36*) and INPE (*23*) are based on Landsat imagery and automatic detection techniques that also include forest as a land cover class. These digital deforestation datasets were used to create masks of forest and non-forest cover classes (deforestation, secondary re-growth, savannah, clouds, shadows, and water bodies) for all Landsat scenes used in this analysis. We masked out non-forest areas from all Landsat images used in this analysis. Selective logging and burned area datasets for 1992, 1996, and 1999 for the

entire Brazilian Legal Amazon were also published in earlier assessments (*24*) and revised here. Datasets for other years in this time series analysis were produced new in this assessment.

Method of Analysis

A time series analysis was conducted using periodic observations at intervals of 3-4 years. It usually takes 4 years to lose the canopy signature in remote sensing of canopy degradation from selective logging or understory burned area (*24,27*). Each observation period is one full year and is referred to as the *observation year* (OY).

This method has been reported in *(24-27, 28)* and for other similar applications *(37,38)*.We applied (*24,27*) to detect selectively logged forests in the Brazilian Legal Amazon for a long time series from 1992 to 2014 with 7 years of observation, in which 1992, 1996, and 1999 were conducted by (*24*) and new to this analysis for 2003, 2006, 2010, and 2014. To select image path-row combinations for analysis we visually inspected each Landsat scenes for the entire Legal Amazon using a band composition RGB near infrared/middle infrared/red (*24,27*). To make an initial inventory of logging locations using heads-up digitizing we delimited visible forest canopy disturbance indicators (e.g. logging patios and roads). Scenes showing visible evidence of selective logging were analyzed subsequently using a semi-automated technique to detect and map selective logging forest areas. The method developed in (*25*) uses a semi-automated technique consisting of the application of a textural algorithm (variance with a 5x5 moving window) on band 5 of Landsat-5 TM or band 6 of Landsat-8 OLI with non-forests areas masked out. It then applies an extended 3-pixel non-forest mask to remove border effects on textural images. These images were used to detect logging lands (patios and roads) and then re-classified using a binary system where 1= patio and 0=forest. Finally, we applied a variable buffer zones (180 and 450 m) around logging lands to estimate the amount of forest land affected by logging activities, but not necessarily visible on satellite images. Digital texture analysis and visual interpretation analysis of selective logging in forests were merged to remove areas that could lead to double counting.

To assess understory burning in Landsat digital images, we applied spectral mixture analysis (SMA) to derive end members for vegetation, non-photosynthetic vegetation, shadow, and bare soil fraction images. This method was developed and described in (*27*) and referenced in (*24,28*). It was deployed using the ERDAS IMAGINE® 2016 software toolset. The combination of selective logging activities and fire were estimated by overlapping the areas of selective logging and burned forests detected within each year. Forest areas common to both logging and fire were classified as areas of selective logging and burn.

To supplement the visual object analysis field reconnaissance datasets were used from field studies in the states of Acre, Rondônia, Mato Grosso, and Pará in July 2002, June 2005, and September 2016 in forest sites showing signs of selective logging and burned area. Several burned forests detected on satellite images were visited and inspected in the field. Logging activities were dated through interviews with the local forest owners and double checked on our logging classification. Logging and fire field data were used to improve visual interpretation and semi-automatic detection techniques to assess forest impact. In addition, ground control points were acquired using GPS (Global Positioning System) device used in the geometric calibration of the Landsat images.

This analysis only reports degradation from intensive logging or fire and omits low intensity cases. In terms of logging, previous analysis (24-27, *28*) shows we do not detect logging at intensities less than 10 m^3 ha^{-1}. These areas were classified as undisturbed forests for each period of the analysis. Consequently, our estimates of selectively logged and burned forests are slightly conservative since it accounts for only medium and high intensity logging and fire in the Brazilian Legal Amazon.

Six individual digital map layers – deforestation and 5 types of degradation - were stacked at each observation year (OY) to delineate pixel overlay unions of new occurrences, persistent occurrences, overlapping occurrences, and sequential occurrences; we then report only areas of undisturbed forest that were degraded for the first time. Pixels of degraded forest that are persistent in the landscape and observed in the remote sensing mapping in following years are counted only on their first occurrence, since we are documenting degradation of undisturbed forest. For instance, pixels we detected as logged in *both* 2006 and 2010 are only counted in 2006 to keep our analysis internally consistent without double counting (**Fig. S1-S3**). Further, previously degraded forest may not be detectable in later OYs even though the biomass or biodiversity impacts remain. Thus, the "cryptic" nature of degradation with respect to satellite observations also requires that we use a spatial tracking approach.

We distinguish between areas that are only logged or only burned from those that are both logged and burned as three distinct degradation types. We report the newly degraded forest pixel counts and the cumulative degraded forest pixel counts, being sure to subtract any degraded forest pixels that are subsequently deforested, to result in a final quantitative assessment of degraded forests at the end of the time series. Forest edges are mapped only in undisturbed forest adjacent to deforested areas to 120 meters. Edge areas adjacent to logging or burned scars are not counted in the edge counts. In any OY, edges are either newly created, converted by deforestation or persistent from previous years, and these cases can be readily separated using the spatial overlays. Isolated forests created by deforestation are mapped for all undisturbed forest patches between 1 km^2 and 100 km^2 in size. To prevent double counting and report non-overlapping areas of distinct degradation classes, we adopt a tabulation hierarchy as follows: a) undisturbed forest that is logged, b) undisturbed forest that is burned, c) undisturbed forest that is both logged and burned, d) edges that are not burned or logged, e) isolated forest fragments that are not logged, burned, nor located in edges (**Table S1**).

Detection Limits and Types of Logging Being Mapped.

The method for detection of logging areas maps areas with harvest removals greater than 10 m^3 ha^{-1}. This is based on our field observations and accuracy assessments. This means we can detect most intensive logging but perhaps miss some low intensive reduced impact logging. In the Amazon, reduced impact logging removes 8-15 m^3 ha^{-1}. More conventional, timber stand improvement logging operations aim to remove 30-35 m^3 ha^{-1}, while conventional industrial logging can remove up to 45-50 m^3 ha^{-1}. We do not map logging that occurs during the process of deforestation where selective trees are culled prior to clearing, nor do we map small holder or homestead-based selective harvests.

Important Reference to Prior Work for Description of Methods and Accuracy Assessment

The methods used in this new analysis of Landsat data for detection of logging and understory burned areas in 2003, 2006, 2010 and 2014 are the same as have been described in detail in

previous publications. (*24-27, 28*) provides a detailed description of the method for logging detection, including the stepwise semi-automated technique and the visual digital object analysis. It also provides results of field-based accuracy assessment of the method. (*25,27*) describe the specific method using a test site in Mato Grosso state. This paper reports details on Landsat image preprocessing for radiometric and geometric calibration. It also provides a detailed description of the remote sensing approach, derivation of vegetation indices and the spectral mixture analysis, including end member selection. It provides a description of the logging and burned area detection. Field validation is also described in (*28*) which provides a detailed description of the method for an Amazon-wide analysis of logging and burned areas. This includes a description of the Landsat data selection process, including logging detection using a semi-automated detection based on texture analysis and a visual digital object algorithm. The logging method includes development of vegetation indices for a fractional cover product that is described as well. It provides background information and full methodology for the detection of burned areas using the spectral mixture analysis. It also provides field validation results.

Accuracy Assessment

Prior publications provide the accuracy assessment for both logging and burning methods. Reference to these works are (24,*27*). An updated accuracy assessment for recent logging analysis is described in (*28*) using detailed digital image analysis with high resolution (5 m) RapidEye satellite data in high density logging areas in Rondônia, Mato Grosso and Para states. Our results indicate a good accuracy for the selective logging classification technique.

Our tests in (*25*) were the first accuracy assessment of the selective logging detection technique based on texture analysis and visual interpretation combined. This compared results with an inspection on a high resolution Ikonos image acquired in 2000. It estimated 82.9%, 91.2%, and 92.9% of user, producer, and overall accuracy, respectively, to detect selective logging in a study site in the state of Mato Grosso. We updated and confirmed these results (*24*) with estimated an overall accuracy of 92.9% and a kappa statistic of 0.82 by applying semi-automated and visual interpretation techniques combined to detected selective logging in the Brazilian Amazon. Latter studies (*27*) estimated an overall accuracy of 95.8% and overall kappa statistics of 0.91 by applying the same semi-automatic technique combined with visual interpretation to detect selective logging and burned forests in a Landsat scene in the state of Mato Grosso, Brazil.

More recent and more detailed analysis in (*28*) conducted an accuracy assessment of our forest degradation technique in three states (Mato Grosso, Pará, and Rondônia) in the Brazilian Amazon by comparing our semi-automatic classification results using Landsat imagery with eye inspection of high resolution Rapideye imagery. Costa results indicates an overall accuracy of 91%, 93%, and 93% for the states of Mato Grosso, Pará, and Rondônia, respectively.

Use of a Periodic Observation Framework.

This analysis selects the use of a periodic, or synoptic, timing for gathering observations from satellite data on degradation in the forest landscape (*39*). We note that while the observations are periodic, the signal of forest degradation in the landscape is persistent and cumulative, which is the basis for our measurements. An alternative approach would be to gather satellite data for the entire BA each year over the 25-year period of analysis. Some authors have done this on a decade basis such as (7). One concern is that the forest canopy signal from selective logging or burning in the understory might dissipate or disappear sooner than our 3 to 4-year repeat interval

allows. However, we note that using an interannual assessment has its own set of problems including annual timing due to cloud cover constraints, data in availability, phenological differences and other factors. This has been reported to be an issue for INPE's national reporting and provisions are made to take into account data gaps, which results in internal in consistencies in the dataset and difficulties in interpretation of rates compared to the accumulated area deforested. Comparisons between different studies can be difficult on an annual basis as has been well noted by (*12*). The interannual analysis by (7) had to devise an interannual model to account for inconsistencies and data gaps.

Furthermore, we were interested in using an approach that could form the basis for a model which could be used with national REDD programs, not only in Brazil but also elsewhere in closed tropical forest regions, knowing full well that the Brazilian national program has considerable technical capacities. Any method that reduces data demands would seem to be desirable, especially considering that in an analysis such as this the remote sensing processing is only one step in the data analytics. Alignment of spatial data layers on an annual basis presents sliver and fragment polygons and other issues that require interpretation and adjustments. In part our decision to use a 3-4 year synoptic approach rests in the notion that accumulating the signal of degradation over time enhances the numerical detection and analysis by measuring larger areas and the accumulation of differences.

To deploy a periodic model, we benefit form from a long record of previous studies related to (*24-27, 41*). This record has established what we believe to be a well-grounded, tested, and validated method (*24*,*26*) in the BA forests.

(27) have shown that selective logging activities are quite evident in field observations a few years after timber extraction and it can be detected in remotely sensed imagery more than a year after logging. Those authors recommended that selective logging mapping should be conducted between 2 to 3 years after logging to avoid underestimation. An analysis by (*24*) using a spectral mixing model of the type developed by (27) and used here noted difficulties in detection of low intensity logging, such as reduced impact logging, but noted successful detection after 3.5 years. In this current analysis, we tabulated results for seven different observation years (1992, 1996, 1999, 2003, 2006, 2010, and 2014) for measurement and analysis purposes. The average spacing in time is 3.67 years. We report above that we are detecting forest disturbances from logging at extraction rates >10 m^3 ha^{-1}. In (24,27) we note that detection of canopy damages by logging and the burn scar from understory fires is spectrally and visibly detectable at these degradation intensities for 3 to 4 years.

Selectively logged forests were classified into two separate vector coverages: 'obvious' and 'subtle' logging. 'Obvious' logging includes spectrally bright patios, roads, and obvious canopy disturbance. Subtle logging refers to logged areas that exhibit visible canopy disturbance and faded patios or no patios. Forests that did not have visible canopy disturbance on satellite images were not digitized and, therefore, classified as non-logged forests for each period of analysis. Our own work (*28*) conducted an interannual analysis of forest degradation analysis in the state of Mato Grosso. That study estimated an average of 62.5%, 81.1%, and 67.7% of overlap with previously annually detected selective logging only, logged & burned, and burned only, respectively. Based on it, they concluded that selective logging can be detected using Landsat imagery from 3 to 5 years following logging activities and 3 to 10 years following fire events in that study area, which will vary according to the fire and logging intensity and frequency and forest characteristics controlling regeneration capacity.

Mapping of Forest Edges

To estimate forest degradation by edge effects we performed a buffer overlay in a geographic information system on the digital deforestation maps from TRFIC (1992, 1996, 1999) and INPE (2003, 2006, 2010, 2014, 2018). The buffer width specified as 120 m, which is four Landsat pixels in width. Other studies suggest that edge effects may persist into the forest as much as 500 meters or more (*40, 41,42*), so our analysis is conservative with respect to estimated edge-affected area. To compute the edge-affected areas in each observation year, we only tabulate the forest in edges that was not degraded by logging or understory fire. The computation of new edges is derived from the overlay analysis (see below).

Estimation of Isolated Forest Fragments

Isolated forest fragments are patches of forest than range in size from 1 km^2 to 100 km^2. They can be mapped from the deforestation datasets we used (TRFIC digital maps and INPE digital maps). All contiguous areas were identified in the GIS, and the areas measured include all intact forest within the fragment. Forest areas in edges as well as logged or burned forest found inside fragments were not tabulated.

Detected Logged Forest, Burned Forest, Edges, and Isolated Fragments

The areas detected in the imagery or derived from deforestation maps areas shown in **Table S2**. These data represent the total area in the landscape at each observation year that are measured in each degradation type and are represented in **Figure S1** for a selected location in 2006.

Spatial Overlay Change Detection Analysis

Areas of degradation detected at each OY by remote sensing (**Table S2**) are the source for spatial analysis. It is used to identify areas of new degradation created between years of observation (**Table S3**). Spatial analysis is required to make most of the calculations presented in this analysis. It is also used to remove overlapping areas between types of degradation (e.g. logged in forest edges) to ensure that tabulation of total degraded forest area across different types of degradation are not double counted. Overlay analysis is also necessary to determine the interaction between types of degradation and between degradation and deforestation (e.g. the amount of logged forest that is burned, or the amount of logged forest that is deforested).

This spatial analysis is performed using layers of raster datasets for each observation year. We processed five data layers, that include the following: 1) Logged forest, represented as pixels that were classified in the satellite imagery at each year of observation, 2) burned forest, represented as pixels that were classified in the satellite imager at each year of observation, 3) forest edge areas, represented as pixels created by buffering to 120 m from the edge of deforested areas, using the TRFIC and INPE digital datasets of deforestation, 4) isolated forest fragments which are blocks of intact and contiguous forest areas in the digital deforestation datasets from TRFIC and INPE, ranging in size from 1 km^2 to 100 km^2, and 5) deforested areas, represented by the combination of the deforestation and secondary regrowth classes in the TRFIC and INPE digital deforestation datasets. (See **Figure S1**)

To generate an additional data layer for forest areas that were both logged and burned in the same occurrence, the two data layers were merged, creating three separate layers in which specified three forms: logged only, burned only and logged plus burned.

An algorithm was developed that provides a union of all raster data layers. Each pixel is labeled to identify its degradation type and contribution from other merged types (e.g. new logged forest inside a new edge have an identifying label). Then a series of conditional rules are applied as in **Table S1**.

The analysis of conversion of degraded areas by deforestation is another overlay analysis. Areas of detected of logged, burned and logged and burned areas at observation year, t, that overlap with deforested areas at the next observation year, t+1, are tabulated as being converted. Similarly, we can tabulate sequential occurrences of logged, followed by burned, followed by deforestation to evaluate the linkages between these different types of degradation.

Figure S1 shows the results of spatial analysis of remote sensing data for one example observation year of 2006, indicating the coverage of the five forest degradation types, deforested areas and undisturbed forest. Subsequent Figures below show the change detection analysis against this base year.

Tabulation of New Logged, New burned, New Edge and New Isolated Fragments

New logged areas are logged forest areas that were created between observation years (e.g. between 2006 and 2010). These are logged forest that were observed for the first time in the period of observation (e.g. 2010) and do not include preexisting logged areas (e.g. from 2006). These data are different than the inventory of all logged areas detected (**Figures S1-S3)** in each observation year, which may include areas that persist from one observation year to the next or represent re-logging of the same sites. Logged areas are frequently re-logged. We do not tabulate these areas; such repeated logged sites are interesting because they represent a higher degree of impact, but they are not double counted in this inventory. We tabulate understory burned areas in the same way, and do not include re-occurrences. As well, for logging or burning scars that carry forward in images for subsequent years are also not included in the inventory. New edges are edges that were created between observation years and do not include preexisting edges that were maintained through the next observation (e.g. also in 2014). However, we maintain a record of all past new edges that were not deforested in the spatial database for tracking forward in time. Only new isolated fragments are tabulated as with the other forms of degradation. However, we maintain a record of all past new isolated forest.

Figure S2 and **Figure S3** show areas of new degradation by type as well as new deforested areas present in an Amazon landscape in 2006 and in 2010, as a result of overlay change detection analysis. This is a representative example of the Amazon landscape during the period of rapid decline in deforestation rates. Several important aspects of forest cover change dynamics are depicted. First, it generally shows the mapping of new degradation and new deforestation for each observation year. Second, it shows clearly that new deforestation areas decline compared to new degradation areas. Third, it shows the large relative contribution of forest degradation as a disturbance in the landscape. Fourth, it shows the distinct, spatially separated occurrence of burned forest compared to logged forest, where burned forest is declining relative to logged forest. Also evident is the rather large number of burned areas occurring on isolated forest fragments, especially in the 2006 observation year.

Estimate of the Cumulative Degraded Forest Reporting in 2014

One important computation is to determine the overall long-term impact of degradation on the current, 2014, Amazon landscape. This is not possible to measure directly from satellite remote sensing image analysis in 2014 because the signature of many forests degraded earlier are not currently observable (i.e. they are cryptic). To measure the current state of degradation in the landscape, which we report in **Fig. 1B** of the main manuscript, we need to use overlay analysis and tabulate forward all occurrences of the various forms of degradation. We only tabulate the first observation of a degraded forest pixel and we maintain separation of the different types of degradation to prevent double counting. We also considered that some degraded forests are deforested and therefore are moved into a different land cover class not included in our degraded classes. For example, logged areas that are deforested before 2014 are not tabulated and mapped in the 2014 landscape. For edges and isolated forest fragments we map the edges and isolated forests that are not overlapping with logged or burned areas in 2014.

Cross-Validation with Other Studies.

We have compared our method and its results to other studies to understand uncertainty. This comparison suggest our method works, but may be a bit conservative. Souza et al. (7) presented an interannual 10-year time series from 2000-2010 of degradation by logging and understory fire, reporting lower rates (0.51-0.62 of our estimates) but similar when we compare to our logging estimates (0.75). On the other hand, our estimates of logged and burned areas are consistently higher than presented in Tyukavian et al. (*12*) based on an annual sampling framework from 2000-2013 in the arc of deforestation (0.15 of our estimate). The difference may be due to the large areas of logging in new frontier areas beyond the traditional deforestation zone where they sampled. Although logging-driven forest degradation has been noted in the early published literature, some of those estimates are unusually high – as much as 200% higher than rates reported here for any period in this analysis *(43)*. Our estimate of detected burned area is lower than Morton et al. (8), 55,960 km^2 yr^{-1} compared to 85,544 km^2 yr^{-1}, which was based on canopy damage assessment across southern Amazonia including areas outside of the BA using a different remote sensing platform (Moderate Resolution Imaging Spectrometer, 250 m resolution). If 15% of the burned area reported in (8) was outside the BA, the two estimates are closer. Our estimates are closer to (8) than three other prominent analyses that used Landsat data (4, *7*, *12*) that were much lower. The general patterns observed using our method are consistent to (*8*): most burned areas are in proximity to edges, a lack of evidence of frequent re-burning and positive fire feedback, and a trend of low rates peaking in 2006-2010 and falling off again.

Supplementary Text

Analysis of Deforestation of Logged and Burned Forest Areas

There is a prominent notion in the peer literature on deforestation and forest degradation in the Brazilian Amazon that selective logging hastens the loss of forest by deforestation. The concept of positive feedback between logging, fire, and deforestation has been promoted (*31,43,44,45*) and examined by (8). Through our comprehensive analysis of a range of degradation types with deforestation, taking a spatial overlay analytical approach, we made a preliminary evaluation of this process. The first line of analysis examines the degree to which logging occurs simultaneously with burning. This is shown by inspecting the satellite imagery for overlapping

occurrences of logged and burned forest. This is represented in **Tables S2** and **S3** and **Fig. 1** which indicates: a) most logging occurs separated from burned areas which also occur isolated from logged sites, and b) the co-occurrence of burned areas in logged areas is low (e.g. between 1% and 13%).

Through overlay analysis of all data layers for all years of observation, we compute the amount of logged areas that are subsequently deforested throughout the time series. These data are presented in **Table S4A**. Only a small fraction of logged sites is subsequently deforested. Similarly, the amount of degraded forest contributing to the pool of new deforested land is also small as shown in **Table S4B.**

Table S5 shows the magnitude of areas that were sequentially logged then burned, leading to deforestation. This table presents the average annual rate of logged and/or burned areas converted to deforestation based on the detected amounts in each OY. The fractions are not high at any period of the time series and are declining toward the end of the time series, suggesting most burning of logged sites occurs more than 6 years after logging or longer. Less than 24% of logged areas are burned, and less than 16% of logged areas follow the sequence to burning and deforestation at any time in the time series. An examination of logged areas that are subsequently burned by the next time-period is also shown in **Table S5** and is generally around 6% or less. These areas are then compared to the logged areas that were not deforested to compute a fraction. These data suggest that the positive feedback process that hastens deforestation is not an important factor. On the contrary, these and other data from our analysis point to degradation by logging as a distinct form of degradation, and does not couple closely with burning, which is also a separate form of degradation.

There is further evidence from overlay analysis related to the proportion of logged forest occurring within the 120 m wide edges that were mapped here. **Table S6** below shows the fraction, as percent, of detected logged areas found within edges for each year of observation and the fraction, as percent, of burned areas found within the edges. Forest burning is more likely to be close to deforested areas than logged areas.

Survivorship and Persistence of Degraded Forests.

In a similar approach to the analysis of logged and burned areas provide above, we analyzed the survivorship of a given hectare of degraded forest to estimate how long it stays in the landscape before being converted by deforestation. This analysis of persistence is important to understanding whether degraded forest has status as a disturbance regime in the landscape, distinct from deforestation. We tracked each cohort of new degradation by type though its course of time to 2018. We could measure the survivorship to 2018 because we have deforestation data in 2018. These results are shown in the cascading tables below in a series of parts of **Table S7**. At any point in time, the vertical column of results represents the age class distribution at that time, and the diagonals represent the interval survivorship, or age specific survivorship, throughout the time series. Each age specific survivorship varies somewhat, but the general observation is that the age-specific survivorship has increased.

We can focus on some general ages. The short-term survivorship rates (4-8 years) are important because they compare to previous estimates. The long-term survivorship rates ($\geq$15 years) are important because they have not been reported before. We use the entire database to construct average survivorship curves, as shown in **Figure S10.** These vary from any given cohort

survivorship due to generalization. What is clear from the cohort survivorship and the generalized survivorship curves is that logging degradation had a distinctly higher survivorship than the other types, which clustered together at a separate lower level. Furthermore, the slope was less steep, suggesting that logging is particularly persistent in the landscape. Another interesting characteristic of all types is that there is a split at OY 2003, in which it is possible to construct two curves. This is especially true for edges in which a distinct two-curve regression reduces variance considerably.

These results differ from some previous reports that concluded that logging is a precursor to deforestation, while we see that it is not. Further, the fact that burned areas survivorship rates are similar to edges and isolated forest, which are coupled to deforestation rates, suggest that burning is more linked to deforestation than some reports indicate. This analysis of persistence and the analysis of logging, fire and deforestation above suggest that our previous understanding that they are precursors to deforestation is not correct and burning is more closely coupled to deforestation but perhaps not as a direct precursor.

Dominant Type of Local Degradation.

To evaluate the locally dominant driver of degradation, we mapped the type of degradation that had the majority area of all types within a 200 km^2 grid as shown in **Fig. S11 and Fig. 4.** Almost all areas had four types of degradation present, but the mapping aim was to present the dominant one. Unlike our core measure of density (or abundance) which is a measure of the total area of each degradation type, this analysis only reports the type with the largest fraction. Thus, some locations the overall magnitude of the dominant type may have a low total area, while other in another location sub dominant types could be quite high in total area. To present an indication of the relative dominance we presented a map which provides the proportional dominance for each location. For instance, it is possible that in a location with four types of degradation all approximately the same proportion, while at another location the dominant type could be proportionally higher than the next type. The map in **Fig. 4** shows both the dominant type and its proportional representation.

Direction and Trends in Degradation.

The BA was sectioned into several large regions using an overlay grid. For each grid we tabulated the average annual rate new degradation by type and presented it for inter-regional and BA-wide geographical comparisons. The grids generally align with important regions of consideration, but in some cases, we added two grid cells. The annual rates were then divided by the total forest area in 2014 and expressed as a percentage. **Fig. S7-S9** uses the density map as a reference and reports the trend for each type. **Fig. S7** shows the same data but only considering logging and burning. In general, all types of degradation across all regions increase in the first half of the time series. After that, edges and isolated forest rates decline everywhere. Logging rates increase, especially in some notable regions. Burned areas are intermediate, both increasing and decreasing and in some regions of importance for other types is non-existent. It is important to note that these trends differ in magnitude considerably. Regions with high amounts of degradation in the eastern BA decline, while the areas of increasing logging in the western BA are lower in total areas than some high-density logging areas in east and central BA.

Co-Occurrences of Degradation Types.

Because the basic aim of this analysis was to quantitatively and spatially describe the status of the BA today in terms of the area of degraded forest that have occurred since 1992, we tabulated only one instantiation of a degradation type for each record, and used the hierarchical rule provide above. To evaluate the current landscape with respect to the distribution of degraded areas that contained overlapping, or co-occurring, types we analyzed the spatial overlay. **Table S9** shows the results of this overlay. These data take into account all degradation over the entire study period that were not deforested and reports the magnitude of type-only (e.g. area that was only logged, not also burned or found in edges) and the magnitude of various co-occurrences. Unexpectedly, the preponderance of degraded areas that were type-only was very high compared to overlap. This is in part due to our use of a very conservative edge distance. But the basic conclusion is that in 2014 logged areas do not overlap with burned areas nor with edges. If there had been an overlap between a logged area and an edge in the past and that area was deforested it would not be included. So, it is possible that the status of co-occurrences of this type in the past could have been higher than in 2014. Thus, generally each type of degradation can occur in the same landscape, but it is infrequent to exactly overlap, even over time. The general tendency is that logged and burned areas do not overlap with each other concurrently nor over time, and they do not occur in either edges or isolated fragments.

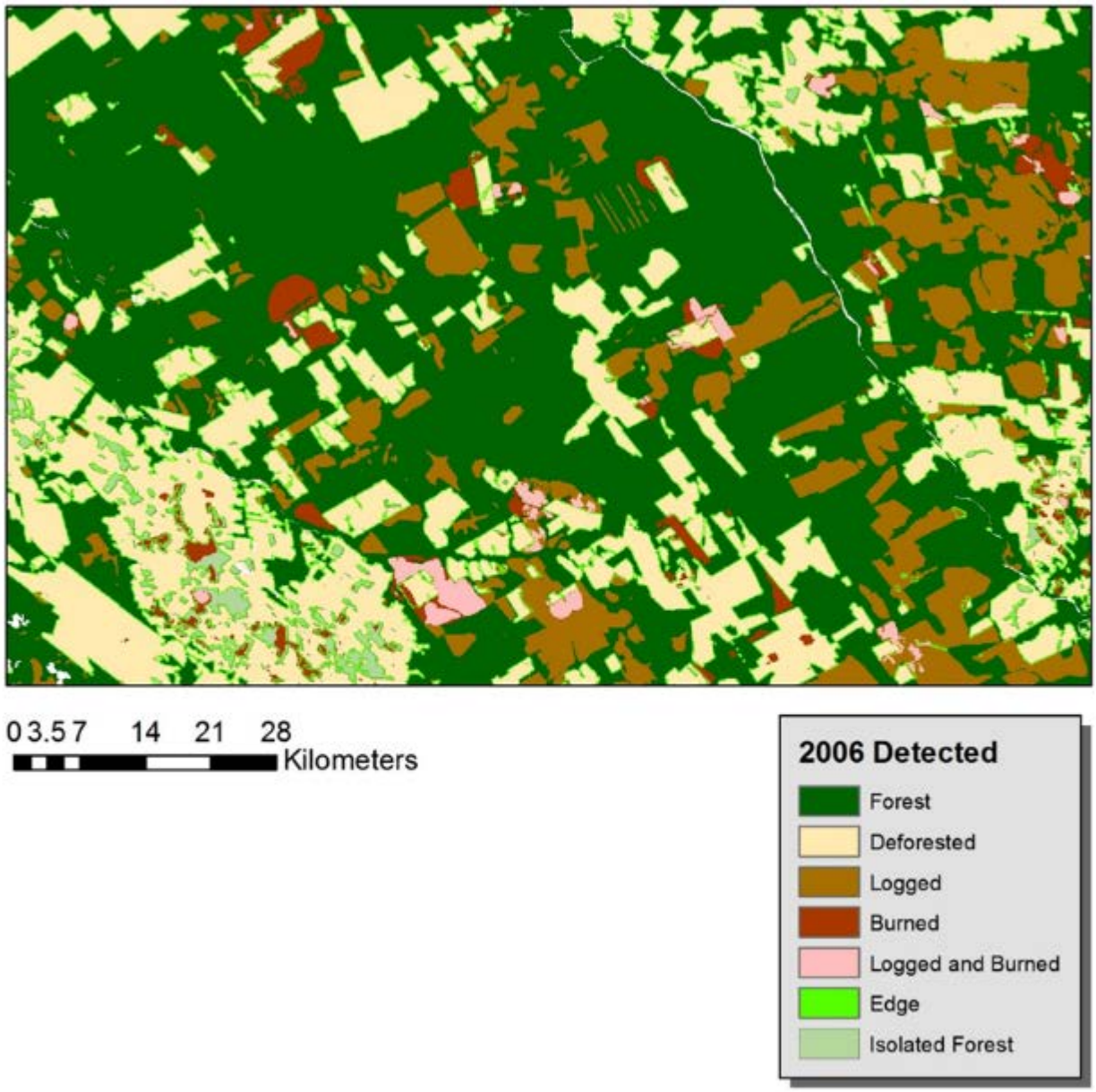

Fig. S1. Representative landscape showing all forms of detected degradation, deforested areas, and undisturbed forest in the observation year 2006.

Fig. S2. Representative landscape showing all forms of new degradation and deforestation from the overlay change detection, including deforested areas, and undisturbed forest in the observation year 2006.

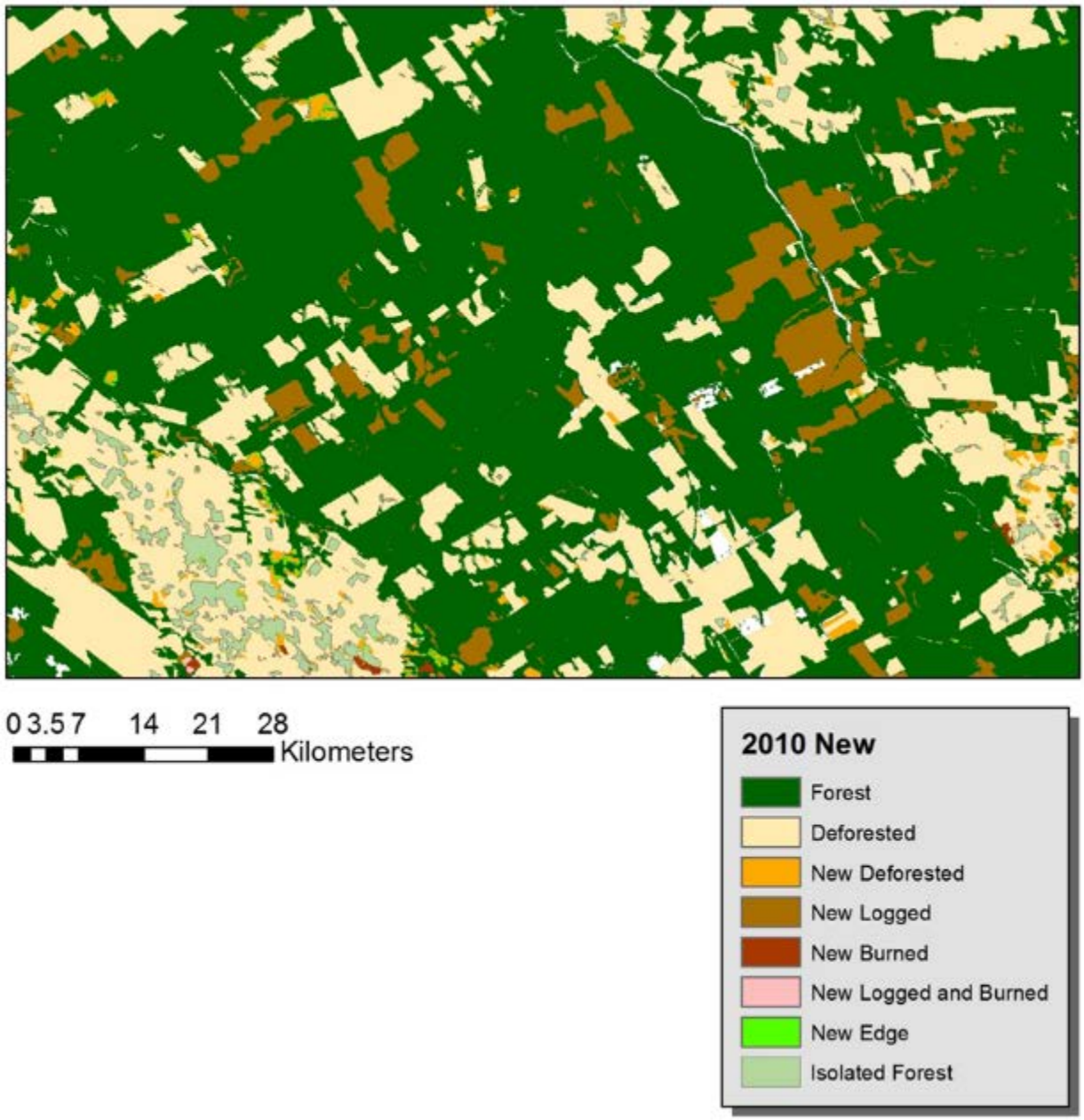

Fig. S3. Representative landscape showing all forms of new degradation and deforestation from the overlay change detection, including deforested areas, and undisturbed forest in the observation year 2010.

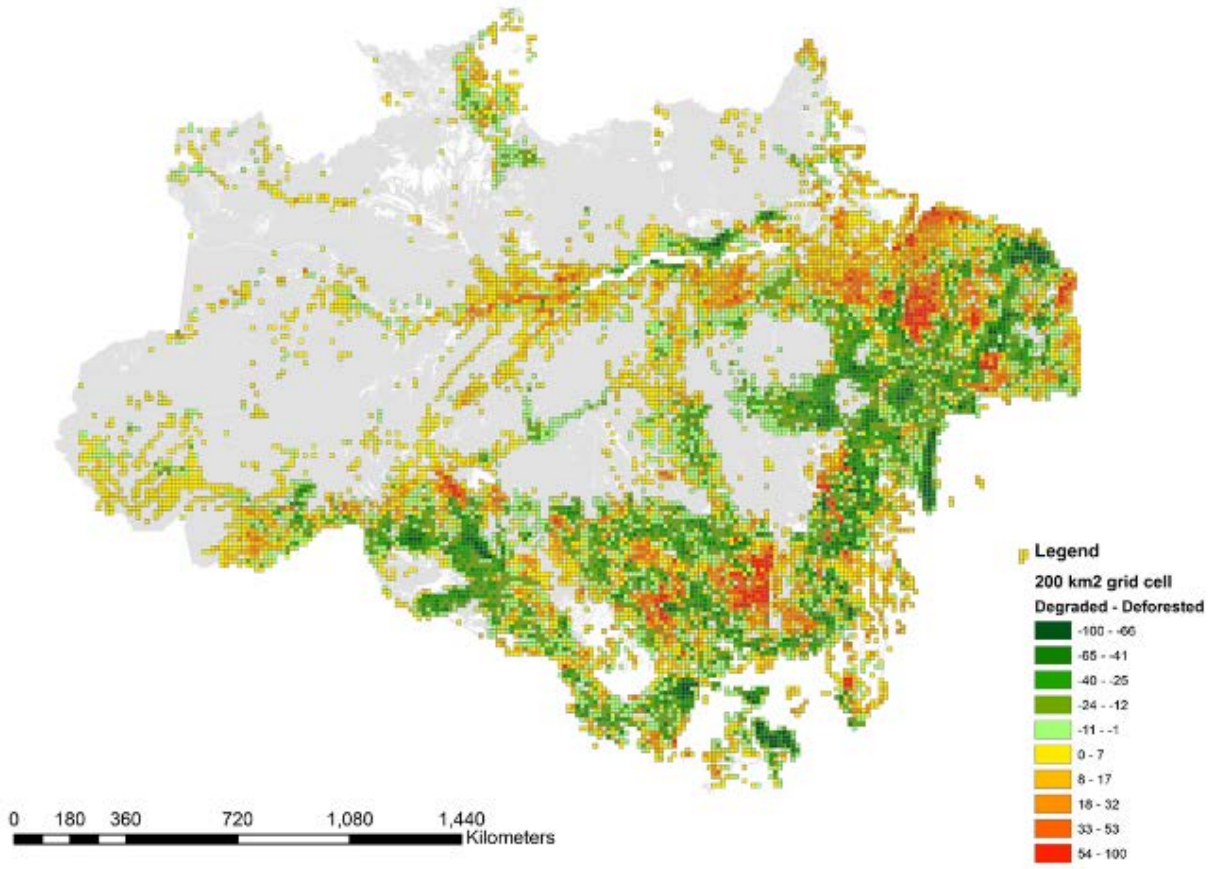

Figure S4. Areas where local degraded area exceeds deforested area. Areas in red shades are local areas where forest degradation covers more area than deforested lands. The values are the difference between area of degraded forest and area of deforested land as a percentage of each 200km^2 grid cell.

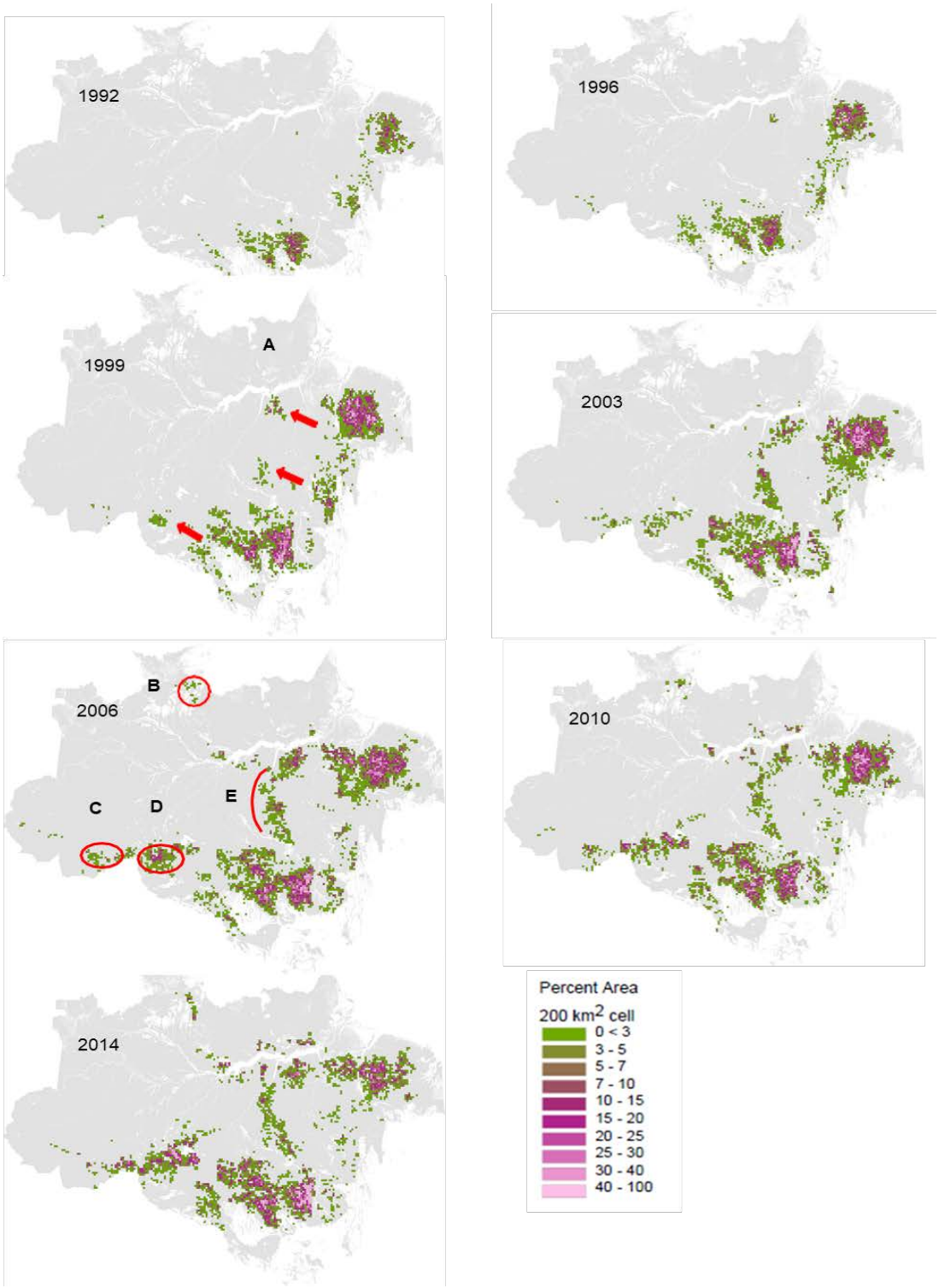

Figure S5. Direction of logging in the BA over time. Detected areas of selective logging at each OY in the analysis. The new western degradation frontier from logging is shown at it initial expansion from the arc of deforestation at A in 1999 progressing to B-E poles by 2006 and later.

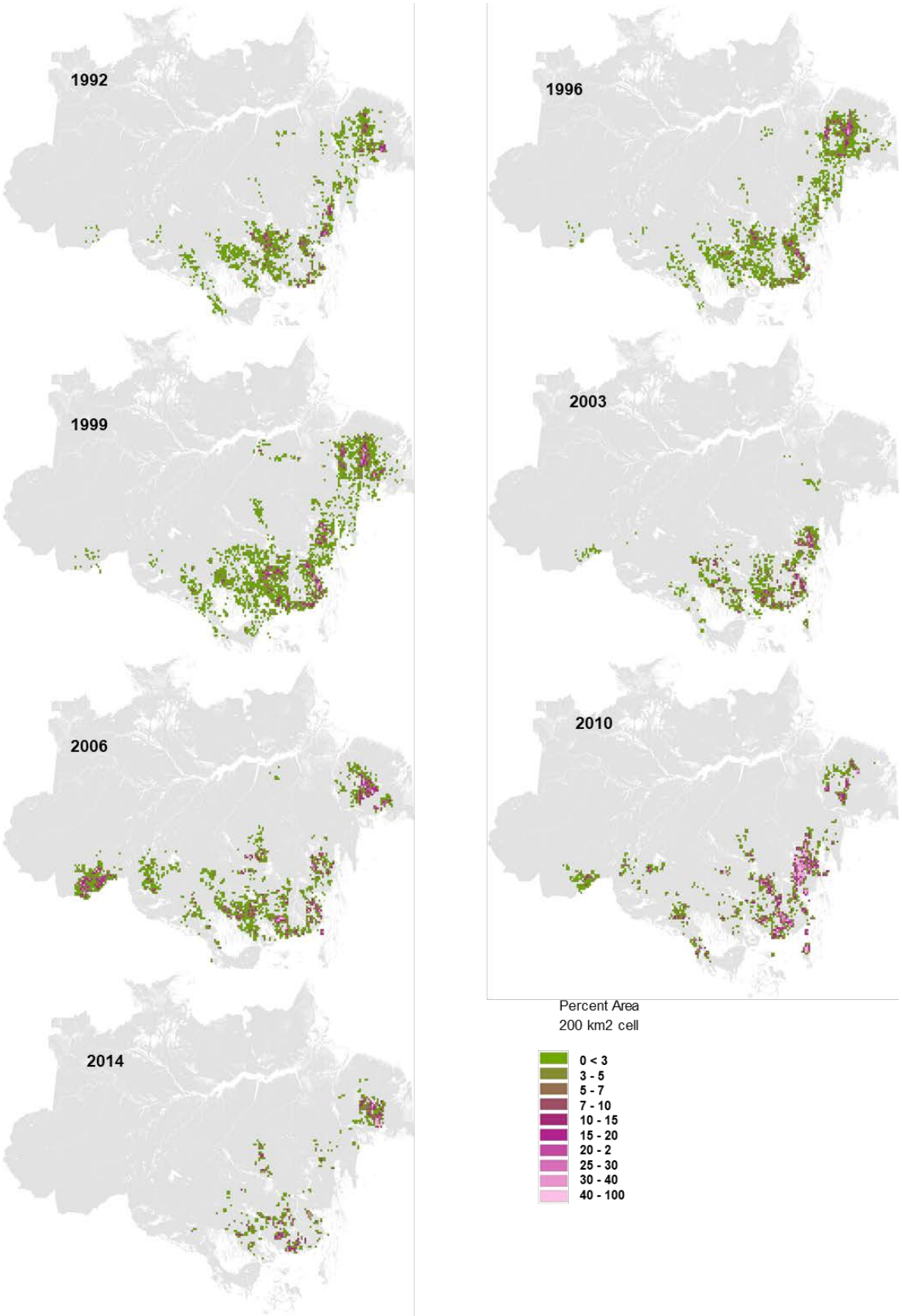

Figure S6. Direction of understory burned areas. Detection of understory burned area over time. Notice that burned areas have declined in recent years, and while they have expanded into the western BA, have closely aligned with the arc of deforestation.

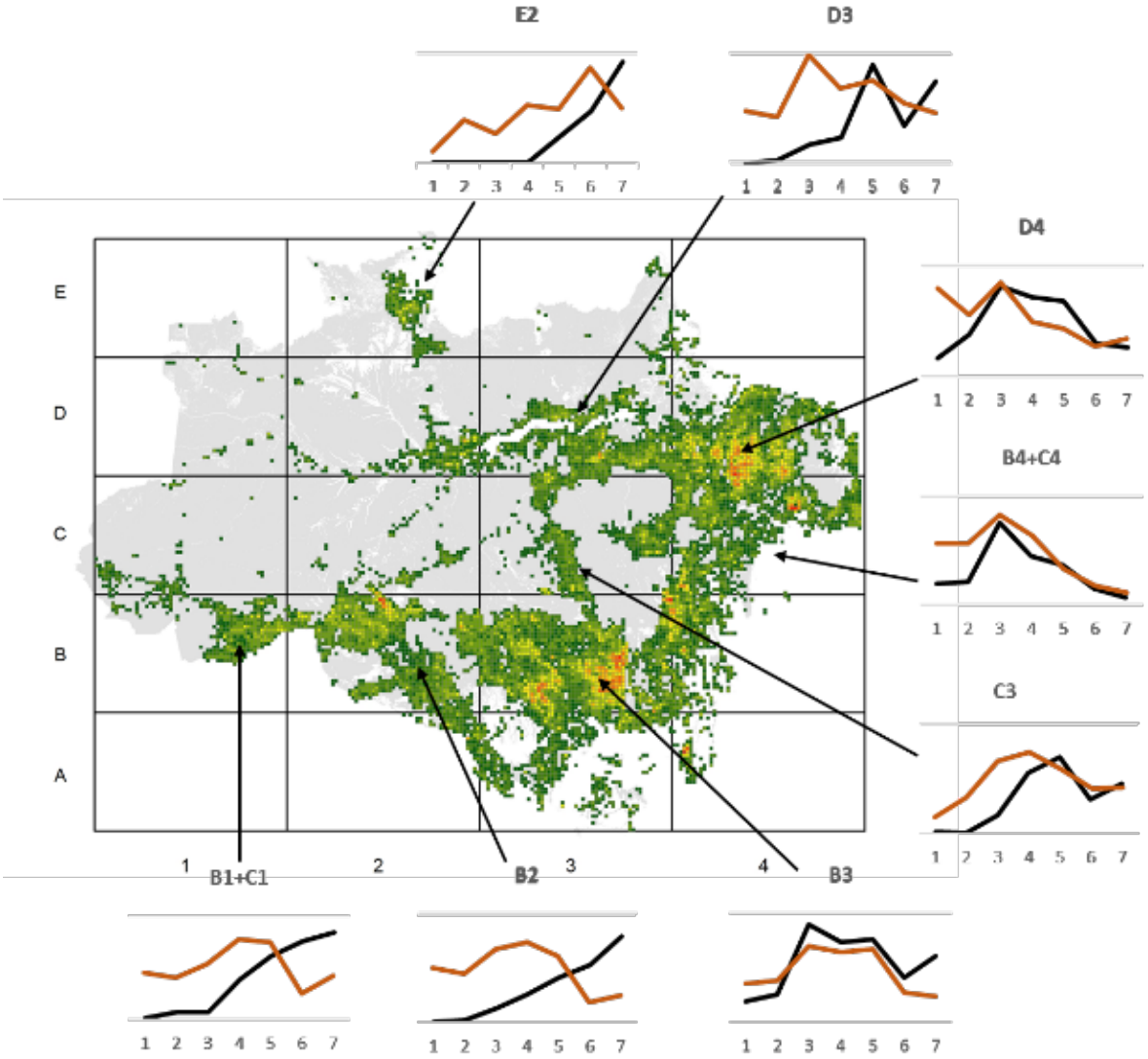

Figure S7. Direction and Trends in Degradation by Logging and Edges in 2014. The map of degradation density is segmented by a large regional grid of generally homogeneous land use change conditions, showing associated trends in new logging (graphic back line) and new edges (graphic brown line) created during the period 1992 to 2014. The scale for each degradation is different and shown schematically here normalized to the maximum rate. See also **Fig. S8-S9**.

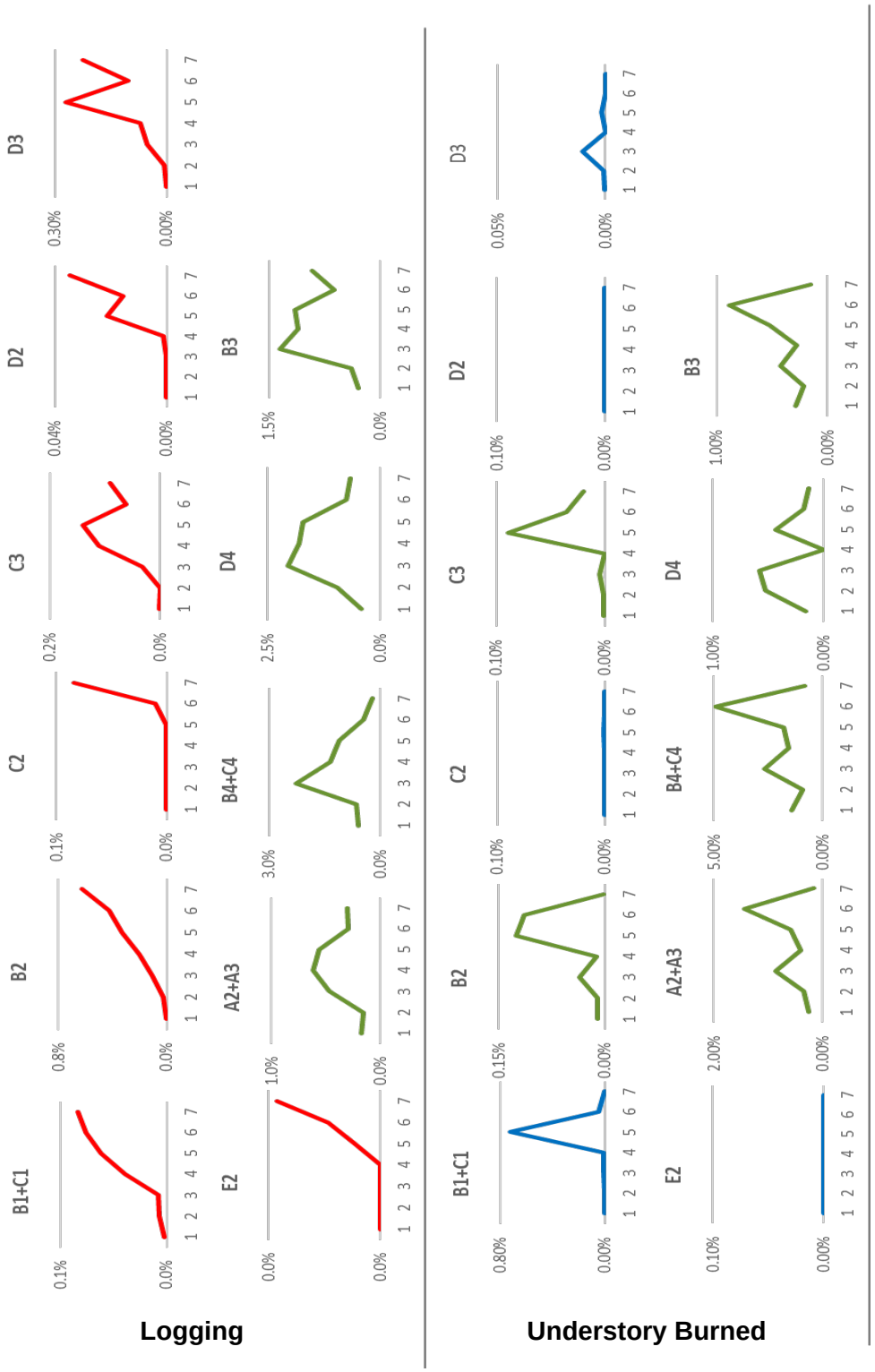

Figure S8. Direction and Trends in Degradation by All Types in 2014. The trend for each type of degradation is shown graphed by large regional grid. grid. Trend lines for each regional grid by logging and burning type. Data are graphed as the new degradation rate as a percentage of the 2014 forest area for the grid, 1992-2014. Red lines indicate increasing trajectory, green lines indicate declining trajectories, and blue lines indicate intermediate or unchanging trajectories.

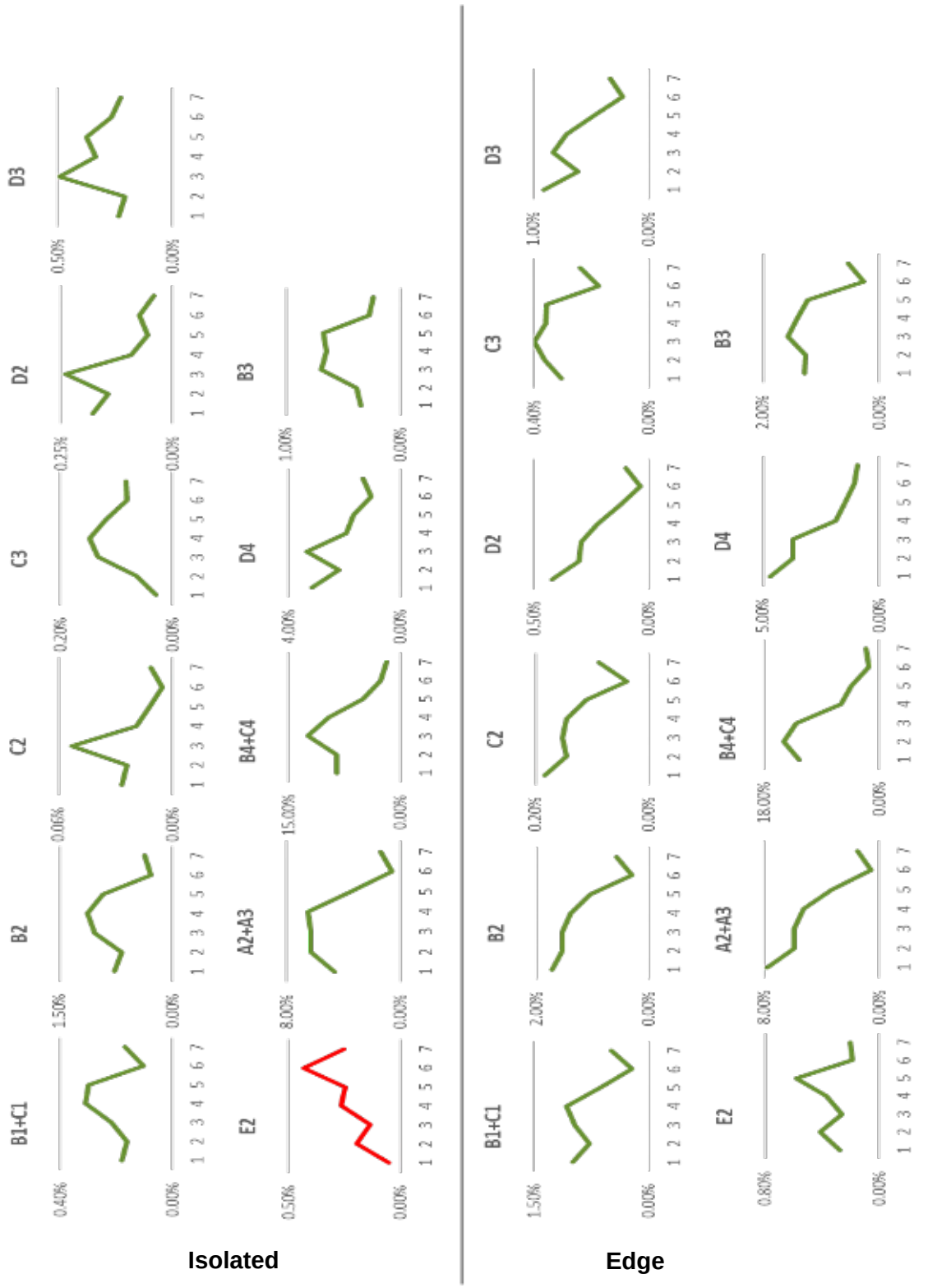

Figure S9. Direction and Trends in Degradation by All Types in 2014. The trend for each type of degradation is shown graphed by large regional grid. grid. Trend lines for each regional grid by isolated and edge type. Data are graphed as the new degradation rate as a percentage of the 2014 forest area for the grid, 1992-2014. Red lines indicate increasing trajectory, green lines indicate declining trajectories, and blue lines indicate intermediate or unchanging trajectories.

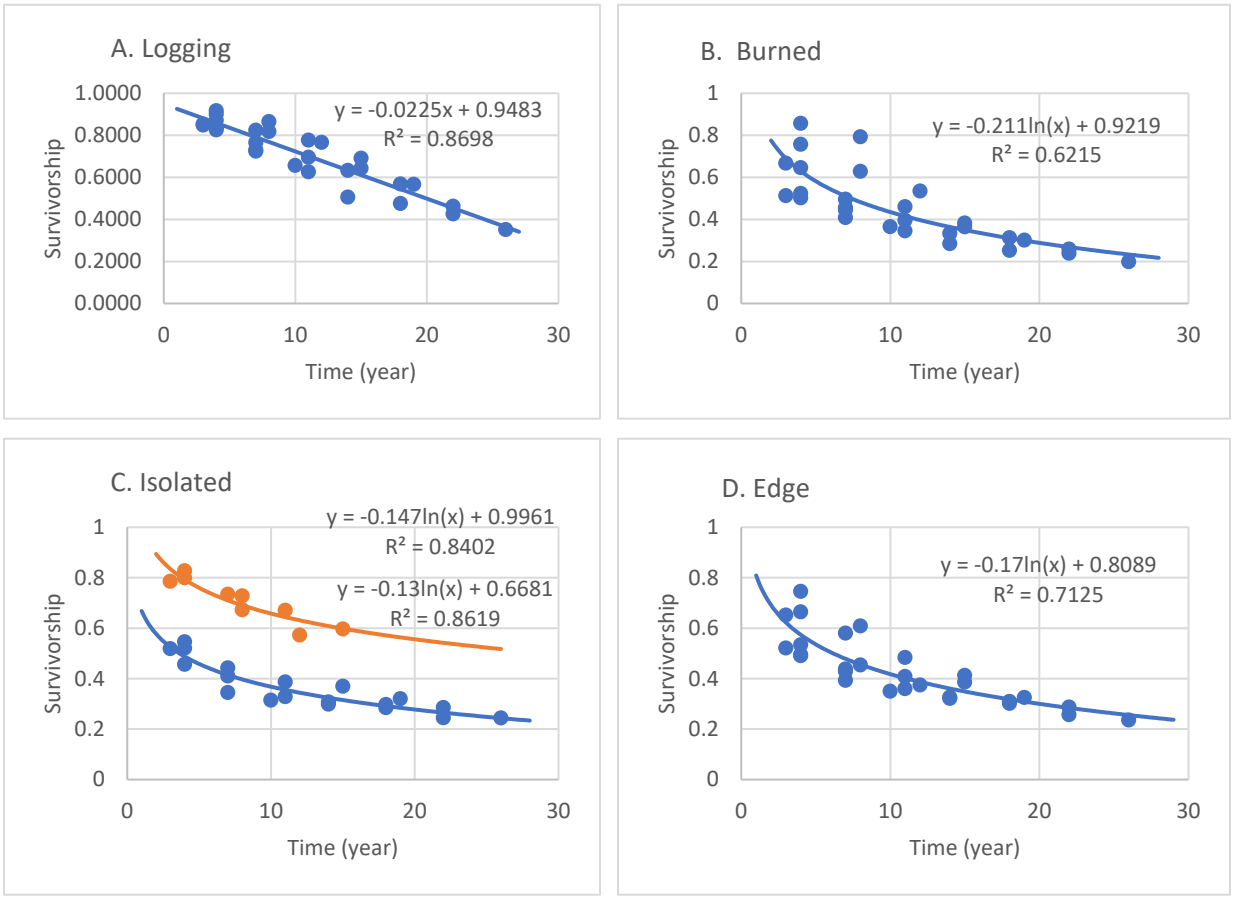

Figure S10. Survivorship curves for four types of forest degradation expressed as x percent after y years since the initial cohort was created as a percentage survival. Isolated forest fragments are shown with plots separated by prior to 2003 (blue) and after 2003 (orange). See Table S7 and S8 for more data on survivorship and persistence.

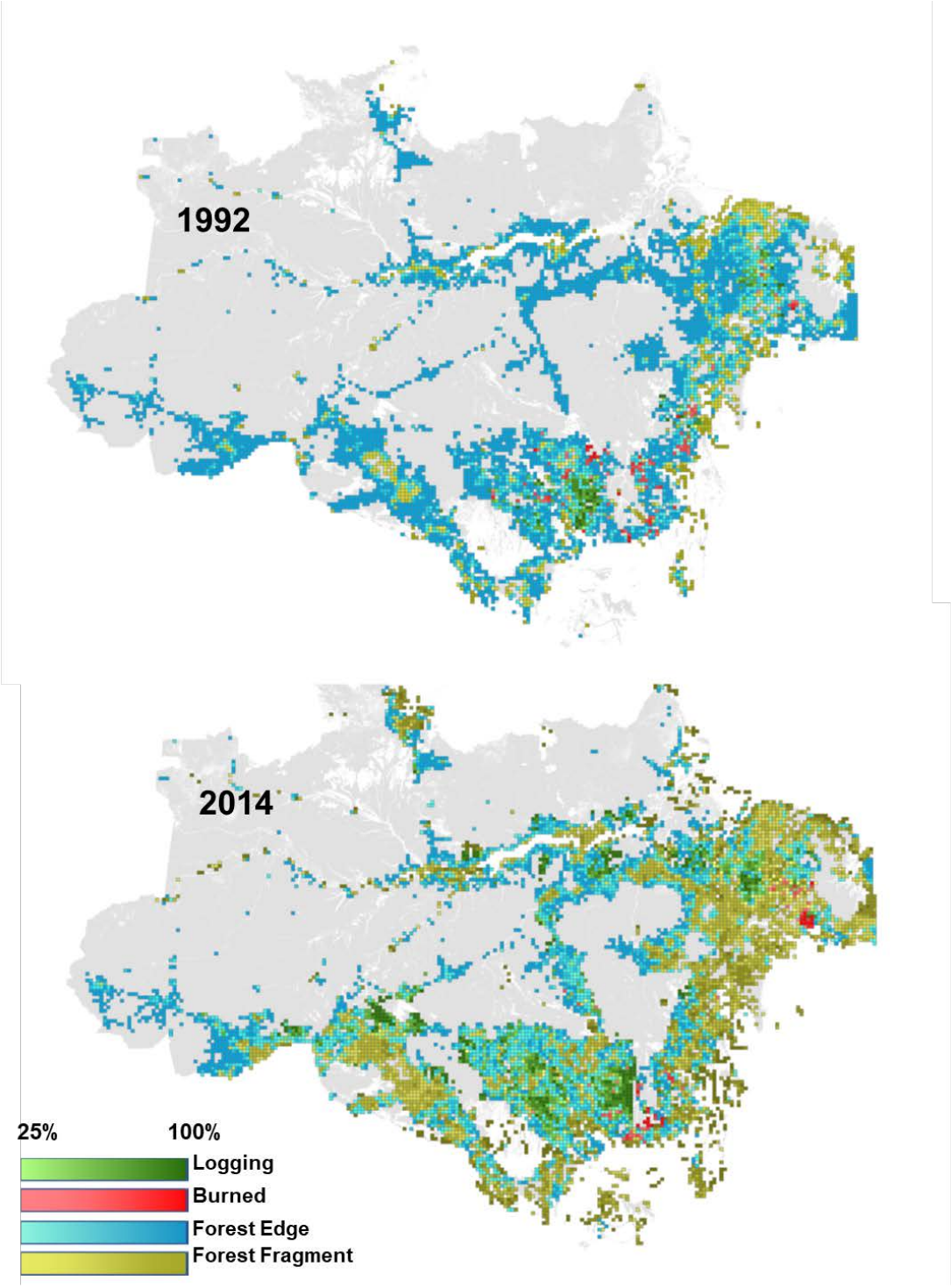

Figure S11. Mapping of the locally dominant type of degradation, with the dominant type shown by color and expressed as the relative percentage of the most dominant type. If all four types were present in equal magnitude the color tone would be close to 25%. A. The dominant driver in 1992 and B. The dominant driver in 2014.

Table S1. Conditional rule protocol for tabulation and mapping of overlay categories of types of forest degradation. The protocol is hierarchical, which gives weight to logging and burned areas, and is used to inventory undisturbed forest that was degraded. Once detected as degraded, it does not get re-inventoried. The initial conditions begin with an inventory of areas 1992.

Degradation type	Code	Condition	Tabulated
New logged	L1	Logged in date, t-1, not logged in date, t	No
	L2	Logged in date, t-1, and logged in date, t	No
	L3	Not logged in date, t-1, logged in date, t	Yes
New burned	B1	Burned in date, t-1, not logged in date, t	No
	B2	Burned in date, t-1, and logged in date, t	No
	B3	Burned in date, t-1, logged in date, t	Yes
New logged & burned	P1	Log+Burned in date, t-1, not logged in date, t	No
	P2	Log+Burned in date, t-1, and logged in date, t	No
	P3	Not Log+Burned in date, t-1, logged in date, t	Yes
New Edges	E1	Edge in date, t-1, not edge in date, t, and not logged or burned or logged and burned in date, t	No
	E2	Edge in date, t-1, and edge in date, t, and not logged, burned or logged and burned in date, t	No
	E3	Not Edge in date, t-1, and edge in date, t, and not logged or burned or logged and burned in date, t	Yes
Isolated Fragments	F1	Isolated fragment in date, t-1, not in date, t, and not logged or burned or burned and logged, or edge in date, t.	No
	F2	Isolated fragment in date, t-1, and in date, t, and not logged or burned or burned and logged, or edge in date, t.	No
	F3	Not isolated fragment in date t-1 and isolated fragment in date, t, and not logged or burned or burned and logged, or edge in date, t.	Yes

Table S2. Forest degradation by type of degradation detected by remote sensing analysis or developed spatially based on digital maps of deforestation in each observation year, 1992-2014 (km^2).

Degradation type	1992	1996	1999	2003	2006	2010	2014
Logged only	5,561	8,888	24,108	33,192	33,665	32,604	39,280
Burned only	5,866	6,425	9,621	5,873	13,896	22,505	6,649
Logged and Burned	390	1,125	1,885	371	1,064	745	431
Edge	116,947	141,108	134,849	116,650	129,628	137,418	138,914
Isolated	32,167	39,458	49,334	63,574	70,348	77,599	83,580
Total Degraded	**160,931**	**197,004**	**219,797**	**219,660**	**248,601**	**270,871**	**268,854**

Table S3. Area estimates of new degradation mapped between observation years and the average annual rates of forest degradation.

(A) Areas of new degradation (area of undisturbed forest degraded) between observation periods, 1992-2014 (km^2).

Forest disturbances	**92-96**	**96-99**	**99-03**	**03-06**	**06-10**	**10-14**
New Logged only	8,498	19,791	25,383	21,109	16,060	22,952
New Burned only	5,290	7,482	4,436	10,070	17,722	3,301
New Logged and Burned	1,078	1,380	277	462	235	74
New Edge	106,902	77,509	78,407	55,251	20,242	23,859
New Isolated	25,179	26,062	32,923	15,493	12,209	8,315
Total New Degraded	**146,947**	**132,224**	**141,426**	**102,385**	**66,468**	**58,501**

(B) Average annual rates of degradation from all types between periods of observation, 1992-2014 (km^2 yr^{-1}).

Forest disturbances	**92-96**	**96-99**	**99-03**	**03-06**	**06-10**	**10-14**
Logging rate	2,124	6,597	6,346	7,036	4,015	5,738
Burned area rate	1,323	2,494	1,109	3,357	4,431	825
Logged and Burned rate	270	460	69	154	59	19
Edge rate	26,725	25,836	19,602	18,417	5,061	5,965
Isolated forest rate	6,295	8,687	8,231	5,164	3,052	2,079
Degradation rate	**36,737**	**44,075**	**35,357**	**34,128**	**16,617**	**14,625**
Deforestation rate	**19,235**	**15,956**	**20,859**	**20,357**	**9,756**	**5,473**

Table S4. The fate of logged and burned areas. The amount annually converted to deforestation and the contribution of these degraded forests to deforestation rates.

(A) Area (km^2 yr^{-1}) and fraction (%) of detected logged and detected burned forest subsequently *converted to* deforestation between observation years.

Type of disturbance	**92-96**	**96-99**	**99-03**	**03-06**	**06-10**	**10-14**	**14-18**
Logged only	168	352	938	1,469	607	526	624
Burned only	701	1,036	1,029	710	951	626	466
Logged + Burned	35	338	189	59	77	46	21
Total	903	1726	2155	2238	1635	1197	1111
Logged only	3%	4%	4%	4%	2%	2%	2%
Burned only	12%	16%	11%	12%	7%	3%	7%
Logged + Burned	9%	30%	10%	16%	7%	6%	5%
Total	8%	10%	6%	6%	3%	2%	2%

(B) Area (km^2 yr^{-1}) and fraction (%) of deforestation that came from degraded forest between observation years, 1992-2018 (km^2)

Land use type	**92-96**	**96-99**	**99-03**	**03-06**	**06-10**	**10-14**	**14-18**
New deforestation	19220	17401	20786	20059	9650	5322	7076
from logging	168	352	938	1469	607	526	624
from burned	701	1036	1029	710	951	626	466
from log + burned	35	113	189	59	77	46	21
% from logging	1%	2%	5%	7%	6%	10%	9%
% from burned	4%	6%	5%	4%	10%	12%	7%
% from log + burned	0%	1%	1%	0%	1%	1%	0%
% from all degradation	5%	9%	10%	11%	17%	22%	16%

Table S5. Detected logged areas that were subsequently burned at *any forward date* in the record and the observed logged areas that were burned in the *next period* (km^2). The reported logged area includes logged areas that were also burned at that time (ie. Logged + burned notation).

Logged forests	**1992**	**1996**	**1999**	**2003**	**2006**	**2010**	**2014**
Total Logged area detected	5,951	10,013	25,993	33,562	34,729	33,349	39,711
Logged, then burned	1,380	2,407	4,526	2,859	2,262	1,323	431
% of Logged area then burned	23%	24%	17%	9%	7%	4%	1%
% of logged area burned and deforested	16%	14%	9%	3%	2%	1%	0%
Logged area burned in the next period	291	615	472	1439	958	546	-
% of logged area burned in the next period	5%	6%	2%	4%	3%	2%	-

Table S6. Fraction of all logged forest and burned forest detected within edges at each OY, %.

Type of forest fraction	1992	1996	1999	2003	2006	2010	2014
Fraction of logged areas within edge	5%	6%	9%	5%	4%	5%	3%
Fraction of burned areas within edge	17%	25%	25%	12%	12%	8%	11%

Table S7. Survivorship analysis for each type of degradation. The total area of new degradation is presented as the initial cohort for each OY to the left. Forest remaining at each interval is reported, and the percent survivorship is reported below.

A. New logged area km^2 not deforested								
Total New Logged Area	**Cohort Year**	**1996**	**1999**	**2003**	**2006**	**2010**	**2014**	**2018**
5,951	**1992**	4,971	4,313	3,727	3,013	2,829	2,536	2,091
9,640	**1996**		8,182	7,378	6,329	6,101	5,479	4,463
21,535	**1999**			17,778	15,739	14,985	13,853	12,205
26,156	**2003**				22,314	21,557	20,315	18,081
21,982	**2006**					19,793	19,026	16,839
16,799	**2010**						15,408	13,747
23,399	**2014**							20,394
							76,618	**87,820**
New logged area not deforested % of originally detected								
		1996	**1999**	**2003**	**2006**	**2010**	**2014**	**2018**
	1992	84%	72%	63%	51%	48%	43%	35%
	1996		85%	77%	66%	63%	57%	46%
	1999			83%	73%	70%	64%	57%
	2003				85%	82%	78%	69%
	2006					90%	87%	77%
	2010						92%	82%
	2014							87%
B. New burned area km^2 not deforested								
Total New Burned Area	**Cohort Year**	**1996**	**1999**	**2003**	**2006**	**2010**	**2014**	**2018**
6,257	**1992**	3,143	2,554	2,160	1,781	1,579	1,492	1,243
6,586	**1996**		3,379	3,001	2,404	2,194	2,058	1,705
9,481	**1999**			6,127	4,210	3,748	3,456	2,857
5,347	**2003**				3,569	2,654	2,463	2,048
13,238	**2006**					10,022	8,322	7,077
19,853	**2010**						17,014	15,739
4,870	**2014**							2,549
							34,805	**33,218**
New burned area not deforested, % of originally detected								
		1996	**1999**	**2003**	**2006**	**2010**	**2014**	**2018**
	1992	50%	41%	35%	28%	25%	24%	20%
	1996		51%	46%	36%	33%	31%	26%
	1999			65%	44%	40%	36%	30%
	2003				67%	50%	46%	38%
	2006					76%	63%	53%
	2010						86%	79%
	2014							52%

C. New forest edge area km^2 not deforested								
Total New Forest Edge Area	**Cohort Year**	**1996**	**1999**	**2003**	**2006**	**2010**	**2014**	**2018**
118,646	**1992**	63,268	50,822	42,657	38,066	35,782	34,015	27,949
110,754	**1996**		57,698	43,499	38,718	36,140	34,200	28,403
83,328	**1999**			41,174	36,475	33,998	32,140	27,089
81,350	**2003**				52,980	47,173	39,340	33,535
49,431	**2006**					36,846	30,068	18,516
23,107	**2010**						15,350	10,488
35,022	**2014**							17,168
							185,113	**163,148**
		New forest edge area not deforested, % of originally detected						
		1996	**1999**	**2003**	**2006**	**2010**	**2014**	**2018**
	1992	53%	43%	36%	32%	30%	29%	24%
	1996		52%	39%	35%	33%	31%	26%
	1999			49%	44%	41%	39%	33%
	2003				65%	58%	48%	41%
	2006					75%	61%	37%
	2010						66%	45%
	2014							49%
D. New isolated forest area km^2 not deforested								
Total New Isolated Area	**Cohort Year**	**1996**	**1999**	**2003**	**2006**	**2010**	**2014**	**2018**
57,469	**1992**	31,335	25,425	18,871	17,668	17,086	16,365	14,014
54,350	**1996**		28,159	18,725	17,072	16,214	15,451	13,265
60,061	**1999**			27,387	24,610	23,209	22,175	19,209
64,865	**2003**				50,937	47,602	43,470	38,684
34,446	**2006**					28,488	25,055	19,711
24,593	**2010**						19,653	16,538
23,629	**2014**							12,284
							142,168	**133,705**
		New isolated forest area not deforested, % of originally detected						
		1996	**1999**	**2003**	**2006**	**2010**	**2014**	**2018**
	1992	55%	44%	33%	31%	30%	28%	24%
	1996		52%	34%	31%	30%	28%	24%
	1999			46%	41%	39%	37%	32%
	2003				79%	73%	67%	60%
	2006					83%	73%	57%
	2010						80%	67%
	2014							52%

Figure S8. The persistence of degraded forest, A) new logged and B) new understory burned forest that was deforested by 2018. C) The total degraded forest deforested by 2018.

A. New logged areas converted to deforested by 2018							
	1992-base	**1996**	**1999**	**2003**	**2006**	**2010**	**2014**
Area Deforested	3,406	3,945	7,733	6,160	3,266	1,679	1,482
Area remaining forest	2,091	4,463	12,205	18,081	16,839	13,747	20,394
Total logged area	5,951	9,640	21,535	26,156	21,982	16,799	23,399
Deforested by 2018	57%	41%	36%	24%	15%	10%	6%
B. New Burned areas converted to deforested by 2018							
	1992-base	**1996**	**1999**	**2003**	**2006**	**2010**	**2014**
Area Deforested	4,672	4,468	6,025	2,958	4,653	3,195	1,224
Area remain forest	1,243	1,705	2,857	2,048	7,077	15,739	2,549
Total burned area	6,257	6,586	9,481	5,347	13,238	19,853	4,870
Deforested by 2018	75%	68%	64%	55%	35%	16%	25%
C. New LBEP areas converted to deforested by 2018							
	1992-base	**1996**	**1999**	**2003**	**2006**	**2010**	**2014**
Area Deforested	102,455	79,848	60,994	57,352	33,063	11,839	9,241
Area remain forest	41,306	40,378	48,105	67,686	46,272	39,151	36,930
Total degraded area	160,824	140,911	123,505	132,214	90,039	57,739	51,042
Deforested by 2018	64%	57%	49%	43%	37%	21%	18%

Table S9. Co-occurrences of different types of forest degradation in the 2014 landscape. A. Distribution of co-occurrences. B. Fraction of the total area of a type represented by a combination of types.

A. Co-occurrences			**B. Type of Degradation**	
	Area km^2	**% Area**	**Type**	**Fraction**
Logged	83,513	25%	Only logged	81%
Burned	23,874	7%	Logged and burned	4%
L+B	4,302	1%	Logged and edge	7%
Edge	127,093	38%	Logged and isolated	5%
L+Edge	6,945	2%	Only burned	56%
B+Edge	5,160	2%	Burned and logged	11%
L+B+Edge	1,351	<1%	Burned and edge	14%
Isolated	73,991	22%	Burned and isolated	12%
L+Isolated	5,331	2%	Only L+B	61%
B+isolated	4,508	1%	LB and edge	19%
L+B+Isolated	1,359	<1%	LB and isolated	20%
Total	337,427		Only edge	90%
			Edge and logged	5%
			Edge and burned	4%
			Only isolated	87%
			Patch and logged	6%
			Patch and burned	5%

References and Notes

1. J. E. M. Watson, T. Evans, O. Venter, B. Williams, A. Tulloch, C. Stewart, I. Thompson, J. C. Ray, K. Murray, A. Salazar, C. McAlpine, P. Potapov, J. Walston, J. G. Robinson, M. Painter, D. Wilkie, C. Filardi, W. F. Laurance, R. A. Houghton, S. Maxwell, H. Grantham, C. Samper, S. Wang, L. Laestadius, R. K. Runting, G. A. Silva-Chávez, J. Ervin, D. Lindenmayer, The exceptional value of intact forest ecosystems. *Nat. Ecol. Evol.* **2**, 599–610 (2018). doi:10.1038/s41559-018-0490-x Medline

2. B. Mackey, D. A. DellaSala, C. Kormos, D. Lindenmayer, N. Kumpel, B. Zimmerman, S. Hugh, V. Young, S. Foley, K. Arsenis, J. E. Watson, Policy Options for the World's Primary Forests in Multilateral Environmental Agreements. *Conserv. Lett.* **8**, 139–147 (2015). doi:10.1111/conl.12120

3. Ministry of the Environment, Government of Brazil, "ENREDD+: National Strategy for Reducing Emissions from Deforestation and Forest Degradation, and the Role of Conservation of Forest Carbon stocks, sustainable management of forests and Enhancement of Forest Carbon Stocks" (Ministério do Meio Ambiente, Brasilia, 2016); http://redd.mma.gov.br/.

4. A. Baccini, W. Walker, L. Carvalho, M. Farina, D. Sulla-Menashe, R. A. Houghton, Tropical forests are a net carbon source based on aboveground measurements of gain and loss. *Science* **358**, 230–234 (2017). doi:10.1126/science.aam5962 Medline

5. D. I. Rappaport, D. C. Morton, M. Longo, M. Keller, R. Dubayah, M. Nara dos-Santos, Quantifying long-term changes in carbon stocks and forest structure from Amazon forest degradation. *Environ. Res. Lett.* **13**, 065013 (2018). doi:10.1088/1748-9326/aac331

6. M. Longo, M. Keller, M. N. dos-Santos, V. Leitold, E. R. Pinagé, A. Baccini, S. Saatchi, E. M. Nogueira, M. Batistella, D. C. Morton, Aboveground biomass variability across intact and degraded forests in the Brazilian Amazon. *Global Biogeochem. Cycles* **30**, 1639–1660 (2016). doi:10.1002/2016GB005465

7. C. M. Souza Jr., J. V. Siqueira, M. H. Sales, A. V. Fonseca, J. G. Ribeiro, I. Numata, M. A. Cochrane, C. P. Barber, D. A. Roberts, J. Barlow, Ten-Year Landsat classification of deforestation and forest degradation in the Brazilian Amazon. *Remote Sens.* **5**, 5493–5513 (2013). doi:10.3390/rs5115493

8. D. C. Morton, Y. Le Page, R. DeFries, G. J. Collatz, G. C. Hurtt, Understorey fire frequency and the fate of burned forests in southern Amazonia. *Philos. Trans. R. Soc. B* **368**, 20120163 (2013). doi:10.1098/rstb.2012.0163 Medline

9. D. P. Roy, S. S. Kumar, Multi-year MODIS active fire type classification over the Brazilian Tropical Moist Forest Biome. *Int. J. Digit. Earth* **10**, 54–84 (2017). doi:10.1080/17538947.2016.1208686

10. E. N. Broadbent, G. P. Asner, M. Keller, D. E. Knapp, P. J. C. Oliveira, J. N. Silva, Forest fragmentation and edge effects from deforestation and selective logging in the Brazilian Amazon. *Biol. Conserv.* **141**, 1745–1757 (2008). doi:10.1016/j.biocon.2008.04.024

11. M. C. Hansen, P. V. Potapov, R. Moore, M. Hancher, S. A. Turubanova, A. Tyukavina, D. Thau, S. V. Stehman, S. J. Goetz, T. R. Loveland, A. Kommareddy, A. Egorov, L. Chini,

C. O. Justice, J. R. G. Townshend, High-resolution global maps of 21st-century forest cover change. *Science* **342**, 850–853 (2013). doi:10.1126/science.1244693 Medline

12. A. Tyukavina, M. C. Hansen, P. V. Potapov, S. V. Stehman, K. Smith-Rodriguez, C. Okpa, R. Aguilar, Types and rates of forest disturbance in Brazilian Legal Amazon, 2000-2013. *Sci. Adv.* **3**, e1601047 (2017). doi:10.1126/sciadv.1601047 Medline

13. K. Brinck, R. Fischer, J. Groeneveld, S. Lehmann, M. Dantas De Paula, S. Pütz, J. O. Sexton, D. Song, A. Huth, High resolution analysis of tropical forest fragmentation and its impact on the global carbon cycle. *Nat. Commun.* **8**, 14855 (2017). doi:10.1038/ncomms14855 Medline

14. R. A. Houghton, D. L. Skole, C. A. Nobre, J. L. Hackler, K. T. Lawrence, W. H. Chomentowski, Annual fluxes of carbon from deforestation and regrowth in the Brazilian Amazon. *Nature* **403**, 301–304 (2000). doi:10.1038/35002062 Medline

15. A. P. D. Aguiar, I. C. G. Vieira, T. O. Assis, E. L. Dalla-Nora, P. M. Toledo, R. A. Oliveira Santos-Junior, M. Batistella, A. S. Coelho, E. K. Savaget, L. E. O. C. Aragão, C. A. Nobre, J. P. H. Ometto, Land use change emission scenarios: Anticipating a forest transition process in the Brazilian Amazon. *Global Change Biol.* **22**, 1821–1840 (2016). doi:10.1111/gcb.13134 Medline

16. X.-P. Song, C. Huang, S. S. Saatchi, M. C. Hansen, J. R. Townshend, Annual Carbon Emissions from Deforestation in the Amazon Basin between 2000 and 2010. *PLOS ONE* **10**, e0126754 (2015). doi:10.1371/journal.pone.0126754 Medline

17. C. A. Nobre, P. J. Sellers, J. Shukla, Amazonian deforestation and regional climate change. *J. Clim.* **4**, 957–988 (1991). doi:10.1175/1520-0442(1991)004<0957:ADARCC>2.0.CO;2

18. C. A. Nobre, G. Sampaio, L. S. Borma, J. C. Castilla-Rubio, J. S. Silva, M. Cardoso, Land-use and climate change risks in the Amazon and the need of a novel sustainable development paradigm. *Proc. Natl. Acad. Sci. U.S.A.* **113**, 10759–10768 (2016). doi:10.1073/pnas.1605516113 Medline

19. W. F. Laurance, D. C. Useche, J. Rendeiro, M. Kalka, C. J. Bradshaw, S. P. Sloan, S. G. Laurance, M. Campbell, K. Abernethy, P. Alvarez, V. Arroyo-Rodriguez, P. Ashton, J. Benítez-Malvido, A. Blom, K. S. Bobo, C. H. Cannon, M. Cao, R. Carroll, C. Chapman, R. Coates, M. Cords, F. Danielsen, B. De Dijn, E. Dinerstein, M. A. Donnelly, D. Edwards, F. Edwards, N. Farwig, P. Fashing, P. M. Forget, M. Foster, G. Gale, D. Harris, R. Harrison, J. Hart, S. Karpanty, W. J. Kress, J. Krishnaswamy, W. Logsdon, J. Lovett, W. Magnusson, F. Maisels, A. R. Marshall, D. McClearn, D. Mudappa, M. R. Nielsen, R. Pearson, N. Pitman, J. van der Ploeg, A. Plumptre, J. Poulsen, M. Quesada, H. Rainey, D. Robinson, C. Roetgers, F. Rovero, F. Scatena, C. Schulze, D. Sheil, T. Struhsaker, J. Terborgh, D. Thomas, R. Timm, J. N. Urbina-Cardona, K. Vasudevan, S. J. Wright, J. C. Arias-G, L. Arroyo, M. Ashton, P. Auzel, D. Babaasa, F. Babweteera, P. Baker, O. Banki, M. Bass, I. Bila-Isia, S. Blake, W. Brockelman, N. Brokaw, C. A. Brühl, S. Bunyavejchewin, J. T. Chao, J. Chave, R. Chellam, C. J. Clark, J. Clavijo, R. Congdon, R. Corlett, H. S. Dattaraja, C. Dave, G. Davies, Bde. M. Beisiegel, Rde. N. da Silva, A. Di Fiore, A. Diesmos, R. Dirzo, D. Doran-Sheehy, M. Eaton, L. Emmons, A. Estrada, C. Ewango, L. Fedigan, F. Feer, B. Fruth, J. G. Willis, U. Goodale, S. Goodman, J. C. Guix, P. Guthiga, W. Haber, K. Hamer, I. Herbinger, J. Hill, Z. Huang, I. F. Sun, K. Ickes, A.

Itoh, N. Ivanauskas, B. Jackes, J. Janovec, D. Janzen, M. Jiangming, C. Jin, T. Jones, H. Justiniano, E. Kalko, A. Kasangaki, T. Killeen, H. B. King, E. Klop, C. Knott, I. Koné, E. Kudavidanage, J. L. Ribeiro, J. Lattke, R. Laval, R. Lawton, M. Leal, M. Leighton, M. Lentino, C. Leonel, J. Lindsell, L. Ling-Ling, K. E. Linsenmair, E. Losos, A. Lugo, J. Lwanga, A. L. Mack, M. Martins, W. S. McGraw, R. McNab, L. Montag, J. M. Thompson, J. Nabe-Nielsen, M. Nakagawa, S. Nepal, M. Norconk, V. Novotny, S. O'Donnell, M. Opiang, P. Ouboter, K. Parker, N. Parthasarathy, K. Pisciotta, D. Prawiradilaga, C. Pringle, S. Rajathurai, U. Reichard, G. Reinartz, K. Renton, G. Reynolds, V. Reynolds, E. Riley, M. O. Rödel, J. Rothman, P. Round, S. Sakai, T. Sanaiotti, T. Savini, G. Schaab, J. Seidensticker, A. Siaka, M. R. Silman, T. B. Smith, S. S. de Almeida, N. Sodhi, C. Stanford, K. Stewart, E. Stokes, K. E. Stoner, R. Sukumar, M. Surbeck, M. Tobler, T. Tscharntke, A. Turkalo, G. Umapathy, M. van Weerd, J. V. Rivera, M. Venkataraman, L. Venn, C. Verea, C. V. de Castilho, M. Waltert, B. Wang, D. Watts, W. Weber, P. West, D. Whitacre, K. Whitney, D. Wilkie, S. Williams, D. D. Wright, P. Wright, L. Xiankai, P. Yonzon, F. Zamzani, Averting biodiversity collapse in tropical forest protected areas. *Nature* **489**, 290–294 (2012). doi:10.1038/nature11318 Medline

20. M. Pfeifer, V. Lefebvre, C. A. Peres, C. Banks-Leite, O. R. Wearn, C. J. Marsh, S. H. M. Butchart, V. Arroyo-Rodríguez, J. Barlow, A. Cerezo, L. Cisneros, N. D'Cruze, D. Faria, A. Hadley, S. M. Harris, B. T. Klingbeil, U. Kormann, L. Lens, G. F. Medina-Rangel, J. C. Morante-Filho, P. Olivier, S. L. Peters, A. Pidgeon, D. B. Ribeiro, C. Scherber, L. Schneider-Maunoury, M. Struebig, N. Urbina-Cardona, J. I. Watling, M. R. Willig, E. M. Wood, R. M. Ewers, Creation of forest edges has a global impact on forest vertebrates. *Nature* **551**, 187–191 (2017). doi:10.1038/nature24457 Medline

21. M. C. Castro, A. Baeza, C. T. Codeço, Z. M. Cucunubá, A. P. Dal'Asta, G. A. De Leo, A. P. Dobson, G. Carrasco-Escobar, R. M. Lana, R. Lowe, A. M. V. Monteiro, M. Pascual, M. Santos-Vega, Development, environmental degradation, and disease spread in the Brazilian Amazon. *PLOS Biol.* **17**, e3000526 (2019). doi:10.1371/journal.pbio.3000526 Medline

22. D. Nepstad, B. S. Soares-Filho, F. Merry, A. Lima, P. Moutinho, J. Carter, M. Bowman, A. Cattaneo, H. Rodrigues, S. Schwartzman, D. G. McGrath, C. M. Stickler, R. Lubowski, P. Piris-Cabezas, S. Rivero, A. Alencar, O. Almeida, O. Stella, The end of deforestation in the Brazilian Amazon. *Science* **326**, 1350–1351 (2009). doi:10.1126/science.1182108 Medline

23. Instituto Nacional de Pesquisas Espaciais (INPE), Programa de Monitoramento da Amazônia e demais biomas. Desmatamento: Amazônia Legal (INPE, Coordenação Geral de Observação da Terra, 2019); http://terrabrasilis.dpi.inpe.br/downloads/.

24. E. Matricardi, D. L. Skole, M. A. Pedlowski, W. Chomentowski, Assessment of forest disturbances by selective logging and forest fires in the Brazilian Amazon using Landsat data. *Int. J. Remote Sens.* **34**, 1057–1086 (2013). doi:10.1080/01431161.2012.717182

25. E. A. T. Matricardi, D. L. Skole, M. A. Cochrane, J. Qi, W. Chomentowski, Monitoring selective logging in tropical evergreen forests using Landsat: Multitemporal regional analyses in Mato Grosso, Brazil. *Earth Interact.* **9**, 1–24 (2005). doi:10.1175/EI142.1

26. E. A. T. Matricardi, D. L. Skole, M. Cochrane, M. A. Pedlowski, W. Chomentowski, Multi-temporal assessment of selective logging in the Brazilian Amazon using Landsat data. *Int. J. Remote Sens.* **28**, 63–82 (2007). doi:10.1080/01431160600763014

27. E. A. T. Matricardi, D. L. Skole, M. A. Pedlowski, W. Chomentowski, L. C. Fernandes, Assessment of tropical forest degradation by selective logging and fire using Landsat imagery. *Remote Sens. Environ.* **114**, 1117–1129 (2010). doi:10.1016/j.rse.2010.01.001

28. O. B. Costa, E. A. T. Matricardi, M. A. Pedlowski, E. P. Miguel, R. O. Gaspar, Selective logging detection in the Brazilian Amazon. *Floresta Ambient.* **26**, e20170634 (2019). doi:10.1590/2179-8087.063417

29. See supplementary materials.

30. D. L. Skole, M. A. Cochrane, E. A. Matricardi, W. Chomentowski, M. Pedlowski, D. Kimble, "Pattern to process in the Amazon Region: Measuring forest conversion, regeneration and degradation" in*Land Change Science: Observing, Monitoring, and Understanding Trajectories of Change on the Earth's Surface*, G. Gutman, A. C. Janetos, C. O. Justice, E. F. Moran, J. F. Mustard, R. R. Rindfuss, D. Skole, B. L. Turner II, M. A. Cochrane, Eds. (Kluwer Academic, 2004), pp. 77–95.

31. G. P. Asner, E. N. Broadbent, P. J. C. Oliveira, M. Keller, D. E. Knapp, J. N. M. Silva, Condition and fate of logged forests in the Brazilian Amazon. *Proc. Natl. Acad. Sci. U.S.A.* **103**, 12947–12950 (2006). doi:10.1073/pnas.0604093103 Medline

32. W. F. Laurance, J. L. C. Camargo, R. C. C. Luizão, S. G. Laurance, S. L. Pimm, E. M. Bruna, P. C. Stouffer, G. B. Williamson, J. Benítez-Malvido, H. L. Vasconcelos, K. S. Van Houtan, C. E. Zartman, S. A. Boyle, R. K. Didham, A. Andrade, T. E. Lovejoy, The fate of Amazonian forest fragments: A 32-year investigation. *Biol. Conserv.* **144**, 56–67 (2011). doi:10.1016/j.biocon.2010.09.021

33. S. L. Pimm, T. Brooks, Conservation: Forest fragments, facts, and fallacies. *Curr. Biol.* **23**, R1098–R1101 (2013). doi:10.1016/j.cub.2013.10.024 Medline

34. S. L. Pimm, C. N. Jenkins, R. Abell, T. M. Brooks, J. L. Gittleman, L. N. Joppa, P. H. Raven, C. M. Roberts, J. O. Sexton, The biodiversity of species and their rates of extinction, distribution, and protection. *Science* **344**, 1246752 (2014). doi:10.1126/science.1246752 Medline

35. G. Ferraz, G. J. Russell, P. C. Stouffer, R. O. Bierregaard Jr., S. L. Pimm, T. E. Lovejoy, Rates of species loss from Amazonian forest fragments. *Proc. Natl. Acad. Sci. U.S.A.* **100**, 14069–14073 (2003). doi:10.1073/pnas.2336195100 Medline

36. Tropical Rain Forest Information Center at Michigan State University, Deforestation database for the Brazilian Amazon (1992, 1996, and 1999) (2001); www.goeslab.us/amazondata.

37. D. M. Bell, W. B. Cohen, M. Reilly, Z. Yang, Visual interpretation and time series modeling of Landsat imagery highlight drought's role in forest canopy declines. *Ecosphere* **9**, e02195 (2018). doi:10.1002/ecs2.2195

38. R. C. Grecchi, R. Beuchle, Y. E. Shimabukuro, L. E. O. C. Aragão, E. Arai, D. Simonetti, F. Achard, An integrated remote sensing and GIS approach for monitoring areas affected by

selective logging: A case study in northern Mato Grosso, Brazilian Amazon. *Int. J. Appl. Earth Obs. Geoinf.* **61**, 70–80 (2017). doi:10.1016/j.jag.2017.05.001 Medline

39. C. Gómez, J. C. White, M. A. Wulder, Optical remotely sensed time series data for land cover classification: A review. *ISPRS J. Photogramm. Remote Sens.* **116**, 55–72 (2016). doi:10.1016/j.isprsjprs.2016.03.008

40. D. Skole, C. Tucker, Tropical deforestation and habitat fragmentation in the Amazon: Satellite data from 1978 to 1988. *Science* **260**, 1905–1910 (1993). doi:10.1126/science.260.5116.1905 Medline

41. W. F. Laurance, Edge effects in tropical forest fragments: Application of a model for the design of nature reserves. *Biol. Conserv.* **57**, 205–219 (1991). doi:10.1016/0006-3207(91)90139-Z

42. J. R. Malcolm, Edge Effects in Central Amazonian Forest Fragments. *Ecology* **75**, 2438–2445 (1994). doi:10.2307/1940897

43. G. P. Asner, D. E. Knapp, E. N. Broadbent, P. J. C. Oliveira, M. Keller, J. N. Silva, Selective logging in the Brazilian Amazon. *Science* **310**, 480–482 (2005). doi:10.1126/science.1118051 Medline

44. M. A. Cochrane, A. Alencar, M. D. Schulze, C. M. Souza Jr., D. C. Nepstad, P. Lefebvre, E. A. Davidson, Positive feedbacks in the fire dynamic of closed canopy tropical forests. *Science* **284**, 1832–1835 (1999). doi:10.1126/science.284.5421.1832 Medline

45. M. A. Cochrane, Fire science for rainforests. *Nature* **421**, 913–919 (2003). doi:10.1038/nature01437 Medline